JOURNAL OF RHEOLOGY®

A rheological evaluation of steady shear magnetorheological flow behavior using three-parameter viscoplastic models

Martin Cvek, Miroslav Mrlik, and Vladimir Pavlinek

Citation: Journal of Rheology **60**, 687 (2016); doi: 10.1122/1.4954249
View online: http://dx.doi.org/10.1122/1.4954249
View Table of Contents: http://scitation.aip.org/content/sor/journal/jor2/60/4?ver=pdfcov
Published by the The Society of Rheology

A rheological evaluation of steady shear magnetorheological flow behavior using three-parameter viscoplastic models

Martin Cvek, Miroslav Mrlik,[a] and Vladimir Pavlinek

Centre of Polymer Systems, University Institute, Tomas Bata University in Zlin, Trida T. Bati 5678, 760 01 Zlin, Czech Republic

(Received 29 February 2016; final revision received 24 May 2016; published 22 June 2016)

Abstract

Knowledge of the complicated flow characteristics of magnetorheological (MR) suspensions is necessary for simulations, calculations in engineering processes, or designing new devices utilizing these systems. In this study, we employed three constitutive equations (three-parameter models) for an evaluation of steady shear behavior of MR suspensions. The predictive/fitting capabilities of the Robertson–Stiff (R–S) model were compared with the commonly used Herschel–Bulkley (as a reference) and the Mizrahi–Berk models. The appropriateness of the models was examined using rheological data for diluted as well as concentrated MR systems. The effect of magnetic field strength on model fitting capabilities was also investigated. The suitability of the individual models was evaluated by observing correlation coefficient, sum of square errors, and root mean square errors. A statistical analysis demonstrated that the best fitting capabilities were exhibited by the R–S model, while others provided less accurate fits with the experimental data. Therefore, shear stresses and the yield stress predicted according to the R–S equation can be considered as the most accurate under defined conditions in comparison with the Herschel–Bulkley and the Mizrahi–Berk model predictions. We also showed that the consistency index obtained from the R–S model increased with increasing magnetic field and particle concentration, which physically reflected more rigid internal structures generated in MR suspensions upon an external magnetic field. This behavior was indistinguishable when other models were applied.
[http://dx.doi.org/10.1122/1.4954249]

I. INTRODUCTION

Materials containing micron-sized, soft, ferromagnetic particles dispersed in a nonmagnetic medium are widely known as conventional magnetorheological (MR) suspensions. These systems have been widely studied because they can undergo rapid, reversible, and tunable changes of their mechanical properties upon the application of an external magnetic field [1–3]. In the absence of the magnetic field, particles are randomly dispersed in a medium, and the MR suspension behaves almost like a Newtonian fluid. When the external magnetic field is imposed, magnetically polarizable particles rapidly form rigid chain or column-like structures parallel to the magnetic field direction, making a barrier in the flow domain. As a result, the yield stress appears and viscosity increases several orders of magnitude. The microstructure transition in the magnetic field is governed by a level of competition between the magnetic and hydrodynamic forces. This phenomenon is called the MR effect, and due to this attribute, MR suspensions have attracted significant attention in the automotive or other engineering fields. Dampers, brakes, clutches, valves, precise polishing, or even robotic and haptic devices are just some of the examples of their wide applicability [4–7]. Due to a broad range of possible prospective applications, extensive research on the MR suspensions has been performed. Many studies are related to the reduction of common drawbacks of MR suspensions such as poor sedimentation, thermo-oxidative and chemical stabilities, or suspension redispersibility [8–10].

Currently there is great interest in the accurate modeling of the complex flow behavior of these materials. Constitutive modeling is a valuable tool for simulations, calculations in engineering processes, or designing and developing new devices utilizing these systems [11,12]. Most devices execute a straight-line motion, and therefore the MR suspensions are subjected to a shear flow. Studies dealing with steady shear magnetorheology tend to classify MR suspensions as non-Newtonian fluids that behave according to the Bingham plastic [Eq. (1)] or the Herschel–Bulkley (H–B) models [Eq. (2)] [4,11,13–15]. The Bingham equation is the original viscoplastic equation expressed as

$$\tau = \tau_0 + \eta\dot{\gamma}, \tag{1}$$

where τ is the shear stress, τ_0 is the yield stress controlled by the magnetic field strength, the constant of η represents the plastic viscosity of the system, and $\dot{\gamma}$ is the shear rate. The parameters τ_0 and η are obtained from fitting to macroscale experimental measurements [16]. The Bingham plastic model has gained popularity mainly because of its simplicity [17]. However, its accuracy is questionable due to its linear character once the yield stress is exceeded. Recently, it was concluded [14] that the H–B model is more appropriate for MR suspensions especially in the high shear rate region. Replacing constant plastic viscosity with the shear rate-dependent power-law relation the H–B model can be written as

[a]Author to whom correspondence should be addressed; electronic mail: mrlik@cps.utb.cz

$$\tau = \tau_0 + K\dot{\gamma}^n, \tag{2}$$

where K and n are the consistency index and power-law exponent, respectively. The K and n are material parameters related to materials' flow behaviors.

The Casson model is another predictive model reported in magnetorheology [2,18,19]. This two-parameter empirical model was originally proposed to describe the rheology of printing inks. Lately, it was shown that it provides suitable rheological descriptions for materials such as blood or food products [17]. On the other hand, more complex models (containing more parameters) such as the Papanastasiou model [11] have been suggested. However, the use of simpler models is more appropriate for complex computational problems.

The Robertson–Stiff (R–S) model (also known as the Vocadlo model) [Eq. (3)] was proposed to describe the rheological behavior with nonlinear characteristics of bentonite suspensions, cement slurries, or polymer solutions and gels [17,20]. Due to the similar flow behavior of these materials with MR suspensions, we used the R–S model in magnetorheology for the first time. The mathematical expression of the R–S model is a combination of the Bingham plastic and Ostwald de Waele equations

$$\tau = K(\dot{\gamma}_0 + \dot{\gamma})^n, \tag{3}$$

where parameters K and n can be considered similar to those in the H–B model [Eq. (2)], but parameter $\dot{\gamma}_0$ denotes the shear rate correction factor. The term $(\dot{\gamma}_0 + \dot{\gamma})$ is an effective shear rate [21].

We widened the scope of our investigation by using the Mizrahi–Berk (M–B) model [Eq. (4)], which is commonly used in food engineering [22]. Recently, it was proved to be successful in describing the rheology of concentrated xantan gum solutions [23]. The M–B is three-parameter viscoplastic model incorporating the yield stress term, and it can be expressed by the following mathematical formulation:

$$\tau^{\frac{1}{2}} = \tau_0^{\frac{1}{2}} + K\dot{\gamma}^n \tag{4}$$

with all variables defined similarly as in models above.

For the equations above [Eqs. (1), (2), and (4)], the following condition can be applied:

$$\dot{\gamma} = 0, |\tau| < \tau_0. \tag{5}$$

The expression shows that the yield stress must be overcome to initiate deformation or flow of the material [2]. However, there is some discussion [24] whether a true yield stress exists or not. Despite the controversy, the engineering reality of the yield stress is a desirable and useful concept in a whole range of applications, once the yield stress is properly defined. There is no standard procedure to measure a yield stress value. The common technique is an indirect determination involving appropriate rheological models [23,25].

In this study, steady shear rheological experiments with MR suspensions based on different particle concentrations were performed under various magnetic fields, and the obtained flow curves were analyzed. Viscoplastic models (R–S and M–B) commonly used in other research areas have been employed. To the best of our knowledge, these models have not previously been used in magnetorheology. The main objective of this study was to evaluate the predictive/fitting capabilities of these three-parameter viscoplastic models for a rheological data description of MR suspensions, especially in a low shear rate range (up to $250\,s^{-1}$) with an emphasis on its engineering importance. Finally, the predicted dynamic yield stress as a parameter of fitting models was evaluated.

II. EXPERIMENTAL

A. Particle characteristics

Carbonyl iron (CI) particles (BASF Corporation, Germany) were employed as a dispersed phase. Particle morphology was studied using scanning electron microscopy (SEM; Tescan Vega II LMU, Czech Republic) operating at an accelerating voltage 5–10 kV. The porosity of the CI particles was identified via a low-temperature nitrogen adsorption/desorption process using a volumetric instrument (Belsorp-mini II, Bel, Japan) and evaluated based on the Brunauer–Emmet–Teller (BET) analysis. The response of the CI particles to an external magnetic field was measured by vibrating-sample magnetometry (VSM; Model 7407, Lake Shore, USA) on the approximately 200 mg sample in the range of $\pm 780\,kA\,m^{-1}$ at room temperature.

B. Preparation of suspensions

Appropriate amounts of the CI particles were mixed with commonly used silicone oil Lukosiol M200 (Chemical Works Kolm, Czech Republic, dynamic viscosity of 197 mPa s, and density of 0.97 g cm at 25 °C) resulting in MR suspensions with volume concentrations of 7.5, 15, and 30 vol. %, respectively. In order to eliminate moisture content, the silicone oil was dried at 120 °C and under a vacuum of 200 mbar for 48 h prior to use and left to cool down to room temperature in a desiccator. The suspensions were vigorously mixed and then sonicated for 2 min using an ultrasonic device (Sonopuls HD 2070, Bandelin electronic, Germany).

C. Rheological measurements

All steady shear flow measurements were performed on a Physica MCR502 (Anton Paar GmbH, Austria) rheometer in controlled shear rate mode. Uniformity of magnetic field and the wall slip phenomenon as two possible issues related to magnetorheology measurements were considered [26]. The device was equipped with a Physica MRD 170/1 T magnetocell, which was supplied with an electric current up to 1.5 A. This condition ensured sufficient uniformity of magnetic field and thus adequate column-like structure formation [27]. The electric current was correlated to the true magnetic field strength using a Teslameter (Magnet Physic, FH 51, Dr. Steingroever GmbH, Germany). The applied magnetic field strengths were found to be 0–432 kA m^{-1}. The amount of 0.25 ml of the tested MR suspension was placed between a

steel (material characteristics based on DIN 1.0718—11SMnPb30) magnetic plate, which was fixed, and an original commercially available nonmagnetic titanium (material characteristics based on DIN 3.7165—Ti 6Al 4 V) plate (PP20/MRD/TI), while the gap between the plates was set to 0.5 mm. The sample was subjected to shearing in a shear rate range from 0.01 to 250 s^{-1}. A fixed temperature of 25 °C was maintained by a thermostatic device (Julabo FS18, Germany).

Generally, it is known that magnetic geometries provide higher shear stress values when compared to the nonmagnetic ones. Nevertheless, it was shown [28] via Hall probe measurements and finite element simulations that higher stresses measured with magnetic geometries are mostly caused by increased magnetic flux density rather than by a better contact of the particles to the plate surface.

In order to reduce probability of the wall slip, the appropriate magnetic field was imposed for 1 min prior each on-state measurement. As a result, the column-like structures were developed and the normal force increased, which indicated better contact between the particle columns and the geometry. The apparent wall slip, which arises due to particle sedimentation and thus presence of a depleted layer of liquid with lower viscosity, was also minimized, as the particle chains were distributed between the plates [28]. However, relatively low degree of slippage was still possible as the surface of the commercial geometry PP20/MRD/TI was not roughened [29].

The surfaces of both plates were thoroughly cleaned using ethanol prior each measurement. Rheological characterization was carried out with a four-step protocol. (i) First, the suspension was subjected to preshearing at 50 s^{-1} for 1 min. (ii) Second, rheological behavior in the off-state was measured. (iii) Prior to each on-state measurement, an appropriate magnetic field was imposed for 1 min in order to induce oriented structure development, followed by rheological data collection. (iv) After each on-state measurement, the field-induced structures were disrupted at a shear rate of 50 s^{-1} for 1 min.

To ensure the repeatability and accuracy of the measurement, the rheological data were collected three times; the average values were calculated and further used for evaluation [30]. Each measurement was performed with a freshly mixed representative sample. On the recorded rheograms, mathematical models were applied in order to obtain the parameters of utilized models.

III. RESULTS AND DISCUSSION

A. General characterization

Obviously both, particle dimensions as well as their morphology influence the MR response [2,31]. Also roughness of particle surface plays an important role in the interparticle friction, or structuration of the MR suspension and ultimately affects the rheological behavior of the MR suspensions [32]. Therefore, these characteristics of the employed CI were investigated via SEM. Figure 1 illustrates a micrograph of the studied sample. As can be clearly seen, particles

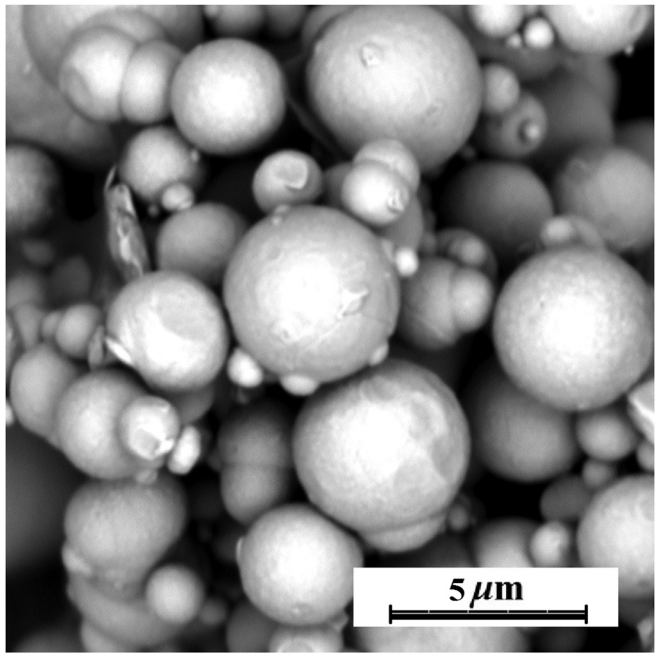

FIG. 1. SEM micrograph of the CI particles.

exhibited almost a spherical shape with quite smooth surfaces a diameter ranging between 1 and 5 μm.

Particle porosity as an important parameter for the calculations of particle volume fraction was determined. If the particles are porous, the final particle density could be significantly affected [32]. However, since the mean pore diameter of the CI particles was approximately 10 nm, it was concluded, that the particles were determined to be compact and therefore, the density value of bulk iron was used for the calculations of the particle volume fraction. A magnetic spectrum of the utilized CI particles was measured. As depicted in Fig. 2, the magnetization curve exhibited the typical shape of a highly magnetizable material, with a low hysteresis, which indicated the appropriateness of the particles for magnetorheology.

B. Rheological measurements

One degree of freedom devices incorporating MR suspensions have been under development since the late 1940s. Their rheological behavior is modeled with the help of classical empirical models, which do not always provide satisfactory data fits [31]. Therefore, the proposal of other viscoplastic models is presented in this study. Conventional steady shear rheological measurements were performed on various formulations of MR suspensions with particular attention paid to low shear rate behavior. The practical importance of modeling is indisputable regarding MR device accuracies, e.g., haptic and force feedback systems which operate at low levels of shear stress [16]. Figure 3 shows the shear rate dependences of the shear stress for prepared MR suspensions under external magnetic fields.

The obtained flow curves exhibited typical characteristics of the MR suspension behavior. In the off-state, the shear stress of the MR suspensions was almost proportional to the shear rate, which corresponds to nearly Newtonian-like

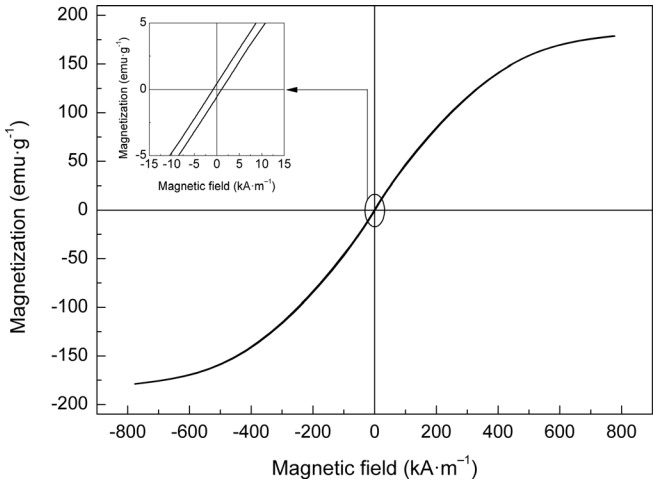

FIG. 2. VSM spectrum of the CI particles. The inset figure displays particle magnetic hysteresis.

behavior. In the on-state, the field-induced structures represented resistance against shearing, and the shear stress increased by several orders of magnitude (up to a factor of 10^4). The on-state shear stress values were strongly dependent on the applied magnetic field strength [2–4]. This property is valuable from a practical point of view as it can provide high performance from MR devices [12]. In general, the highest shear stresses were obtained in the MR suspension based on 30 vol. % particle content. On the contrary, the lowest shear stress values were exhibited by the 7.5 vol. % MR suspension because its oriented particle chains possessed the lowest resistance against shearing.

C. Applicability of viscoplastic flow models and statistical treatment

The obtained experimental data shear stress vs shear rate was fitted with the H–B, the M–B [Eqs. (2) and (4)], and the R–S rheological models. The R–S model was used in its equivalent form [Eq. (6)] [33] in order to obtain parameters

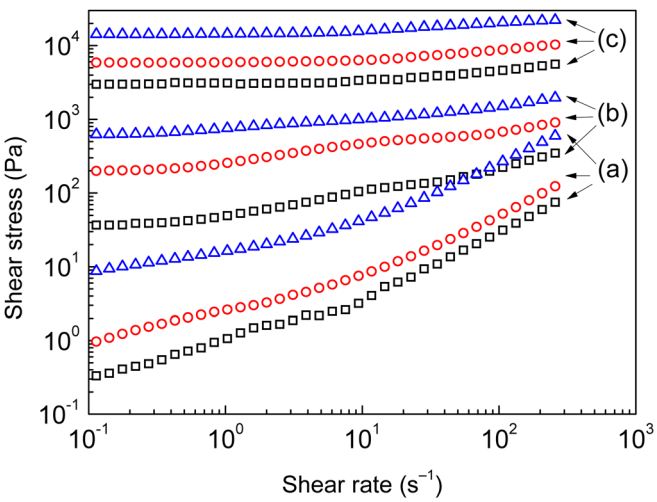

FIG. 3. Rheograms of the MR suspensions containing 7.5 (*open squares*), 15 (*open circles*), and 30 vol. % (*open up-triangles*) of the CI particles at the off-state (a), 72 kA m^{-1} (b), and 432 kA m^{-1} (c) magnetic field strengths.

with a physical meaning applicable for the MR suspensions; hence, the following expression has been used

$$\tau = \left[K^{\frac{1}{n}} |\dot{\gamma}|^{\frac{n-1}{n}} + \left(\frac{\tau_0}{|\dot{\gamma}|} \right)^{\frac{1}{n}} \right]^n \dot{\gamma}. \tag{6}$$

The close fitting of model predictions to the experimental data can be considered according to the coefficient of correlation, (R_C^2), however, this parameter is not totally relevant for nonlinear models [34]. Therefore, it is more appropriate to further evaluate the model inaccuracies by means of the sum of square errors, (SSE), and the root mean square error, (RMSE). These parameters are defined according to the equations

$$\mathrm{SSE} = \sum_i^N (\tau_i - \tau_p)^2, \tag{7}$$

where τ_i and τ_p are observed and predicted shear stresses, and

$$\mathrm{RMSE} = \sqrt{\frac{\mathrm{SSE}}{N-p}}, \tag{8}$$

where N is the number of measurements, and p denotes the degrees of freedom (number of parameters in the rheological model). Thus, the observation of R_C^2, as well as SSE, and RMSE were taken into account in considering the models' applicability. The model that provided the best fit of the data was that with the highest values of R_C^2 and the lowest values of SSE and RMSE. The results of the statistical evaluation are included in the supplementary material [35].

A demonstrational example of the flow behavior (15 vol. % MR suspension at 216 kA m^{-1}) was chosen to graphically present the accuracies of the employed models. As can be seen in Fig. 4, the H–B and the M–B models tend to under-/overestimate shear stress values at a lower/higher shear rate range. On the contrary, the application of the R–S model resulted in a good agreement between the model predictions and the data in the whole shear rate range. These findings are supported with the numerical results outlined in the supplementary material (please see Table S2) [35].

Figure 5 is displayed in order to demonstrate the R–S model capabilities to fit the rheological data collected under various magnetic fields. Clearly, the use of this model provides an excellent close—fitting to the experimental data points, which suggests its suitability and robustness. The performance of other employed models is presented numerically in Tables S1–S3.

The calculated model parameters are listed in Table I. All models revealed viscoplastic behavior, i.e., pseudoplasticity after exceeding a yield stress. The yield stress parameters with respect to flow curves correspond to the intercept on the Y-axis, which is discussed in Sec. III D.

The K parameter reflects the consistency of the system, which in the MR suspensions increases with particle volume fraction and with applied magnetic field strength as a result

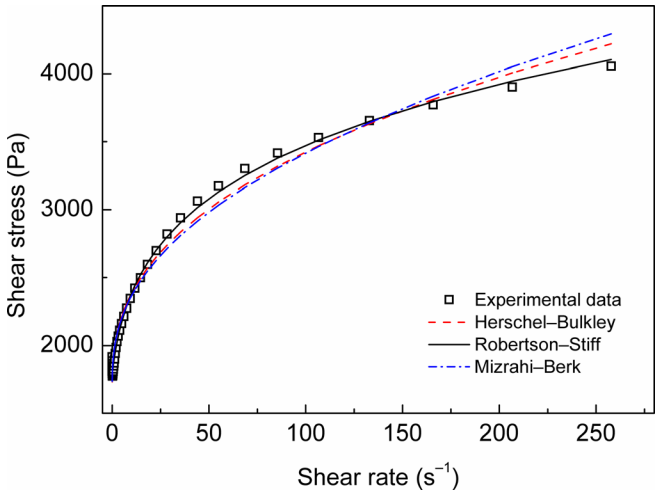

FIG. 4. Shear stress vs shear rate experimental data for a 15 vol. % MR suspension at 216 kA m^{-1} fitted with the H–B (*dashed line*), the R–S (*solid line*), and the M–B (*dashed/dotted line*) models.

of more rigid internal structure formation. This parameter represents such physical meaning connected to consistency only as a parameter of the R–S model. In the H–B and the M–B models, K changed independently on the applied magnetic field. Therefore, the R–S model provided additional information through the consistency index, reflecting the physical property of the MR suspensions upon application of the magnetic field, while the others are from this point of view insufficient.

The n index compares the flow behavior of the MR suspension with a Newtonian fluid. When n equals 1, the fluid behaves according to Newtonian law. The MR suspensions exhibit pseudoplastic attributes, which correspond to $0 < n < 1$. Pseudoplasticity (shear thinning behavior) can be associated with the existence of the field-induced particle structures presented in the MR suspensions. These structures are broken down into smaller aggregates due to intensive shearing and as a result, viscosity decreases. As apparent in Table I, the n is close to 1 as a fitting parameter describing the off-state

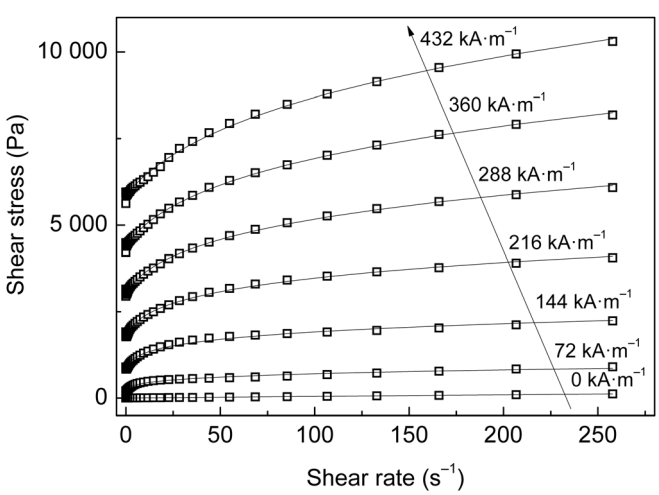

FIG. 5. A representation of the shear stress vs shear rate dependences for the MR suspensions containing 15 vol. % of the CI particles in silicone oil at the off-state, and different magnetic field strengths. The solid lines refer to the R–S model predictions. Model fitting parameters are listed in Table I.

behavior because the column-like structures were not developed. At the on-state, the n index decreased while exhibiting minor differences at various magnetic fields. Thus, it appears that at the on-state, the n represented only an additional parameter, and the rheological characterization was given mainly by combinations of two linear parameters (K, τ_0).

In the M–B model, the conditions for the n parameter are set differently. Newtonian behavior corresponds to n equals 0.5, while pseudoplasticity occurs when $0 < n < 0.5$ as described in [23]. Considering these assumptions, all employed models generally revealed pseudoplasticity in diluted as well as in concentrated MR suspensions, when the external magnetic field was applied.

A statistical analysis of the studied rheological models after fitting in the rheological data of 7.5, 15, and 30 vol. % MR suspensions is summarized in Tables S1–S3. The R–S model in general provided the best correlations and the lowest SSE and RMSE coefficients throughout the whole concentration range as well as magnetic strength range, when compared to other employed models. The values of R indicate that the H–B model also possesses a reasonable predictive/fitting capability, but not as accurate as the R–S model. The M–B model generally exhibited the lowest accuracies (highest RMSE) with the exceptions of the off-state situations for 7.5 and 30 vol. % MR suspensions. To conclude, the flow behavior of the studied MR suspensions was governed by the R–S equation, which demonstrated the best applicability for rheological data description.

The overall suitability of all rheological models (H–B, R–S, and M–B) was further assessed by the evaluation of their RMSE parameters for all concentrations throughout the whole magnetic field strength range. The results of the RMSE analysis are presented graphically by the use of boxplots in Fig. 6. Both the H–B and the M–B models provided similar median values as well as a similar range of the upper quartile and the position of the upper extreme, which informs on their comparable applicability. The use of the R–S model resulted in the lowest median values of the RMSE. Moreover, this model provided the overall best consistency of data values, as its interquartile range is relatively small. The RMSE analysis clearly suggests that the R–S equation provides the best description of the rheological data in the studied MR systems.

D. Yield stress evaluation

Yield stress value cannot be regarded as an absolute material property [24]; however, once it is properly defined, delimited and circumscribed, it is one of the most important rheological characteristics of the MR suspensions. Inaccurate models may result in a shift of the predicted yield stress and, hence, problems with device precision. Therefore, finding the most accurate models is helpful. Low shear rate magnetorheology was used in order to determine flow behavior; the yield stress obtained as a parameter of different viscoplastic models was evaluated.

As illustrated in Fig. 7, the dynamic yield stress increased as a result of the applied magnetic field, which is caused by polarization of the particles that changed the internal

TABLE I. Calculated model parameters for the MR suspensions based on different contents of the CI under various magnetic field strengths.

CI (vol. %)	Magnetic field	0 (kA m^{-1})	72 (kA m^{-1})	144 (kA m^{-1})	216 (kA m^{-1})	288 (kA m^{-1})	360 (kA m^{-1})	432 (kA m^{-1})
7.5					H–B			
	τ_0	1×10^{-5}	32.32	341.5	838.8	1516	2272	3024
	K	0.3569	20.17	142.7	131.78	116.9	114.1	92.12
	n	0.9624	0.4881	0.3134	0.4188	0.5012	0.5433	0.6047
					R–S			
	τ_0	0.5033	37.34	399.9	887.3	1560	2320	3061
	K	0.3109	36.65	419.4	718.0	1016	1317	1540
	n	0.9870	0.3944	0.1785	0.1950	0.2120	0.2206	0.2279
					M–B			
	τ_0	0.2066	27.23	345.0	838.0	1513	2265	3022
	K	0.4552	2.116	3.368	2.219	1.561	1.302	0.8908
	n	0.5202	0.3299	0.2794	0.3798	0.4583	0.4988	0.5663
15					H–B			
	τ_0	1×10^{-5}	126.4	711.6	1686	2938	4313	5714
	K	0.7704	158.6	283.0	278.3	244.0	221.8	287.3
	n	0.9107	0.2797	0.3111	0.3978	0.4729	0.5266	0.4920
					R–S			
	τ_0	1.404	187.6	827.9	1792	3033	4402	5863
	K	0.6222	265.4	865.5	1514	2135	2734	3206
	n	0.9493	0.2120	0.1722	0.1793	0.1897	0.1974	0.2091
					M–B			
	τ_0	0.4340	118.2	713.1	1682	2933	4308	5782
	K	0.7173	5.955	4.776	3.323	2.304	1.763	1.324
	n	0.4779	0.2097	0.2740	0.3599	0.4350	0.4896	0.5453
30					H–B			
	τ_0	1×10^{-5}	601.9	2068	4032	6528	9631	13 598
	K	4.873	157.4	385.1	789.8	961.0	995.1	979.1
	n	0.8643	0.3834	0.3607	0.3131	0.3522	0.3869	0.4081
					R–S			
	τ_0	10.03	654.6	2205	4367	6924	10 049	14 027
	K	3.712	613.3	2 067	4240	6292	8520	11 499
	n	0.9136	0.1991	0.1504	0.1217	0.1307	0.1321	0.1214
					M–B			
	τ_0	5.627	582.6	2064	4028	6517	9618	13 581
	K	1.318	3.484	4.078	5.943	5.818	5.037	4.231
	n	0.5067	0.3142	0.3288	0.2879	0.3248	0.3606	0.3842

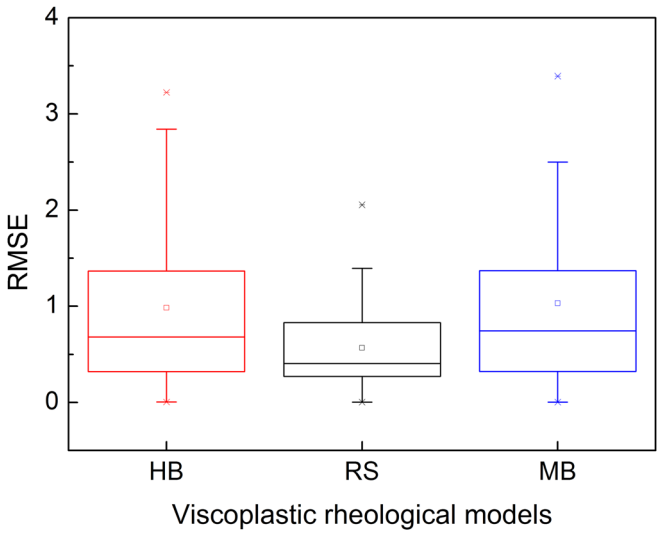

FIG. 6. RMSE boxplots of fitting models for the MR suspensions at a 99% confidence level.

microstructure of the system. Higher yield stresses were attained in the MR suspensions that incorporated larger amounts of particles, because these possess the ability to develop more rigid chain/column-like structures. All models predicted yield stress values in accordance to the polarization model, which suggests its quadratic proportionality with the magnetic field strength. After exceeding a critical magnetic field, H_C, local saturation magnetization of the particles became apparent and yield stress varied only with $H^{1.5}$ [36,37]. The H_C was determined at 250 kA m^{-1}; however, the transition was less noticeable in the MR suspension based on 30 vol. %, probably due to a shifted local saturation magnetization as a result of higher particle volume.

In all the MR suspensions, the highest values of the yield stress were calculated as a parameter of the R–S model. The H–B and the M–B models predicted similar yield stress values; however, some discrepancies were present especially at low magnetic field strengths. Nevertheless, in general, the differences in the yield stress values for corresponding magnetic field strengths obtained via employed models were less than 10% in all studied suspensions.

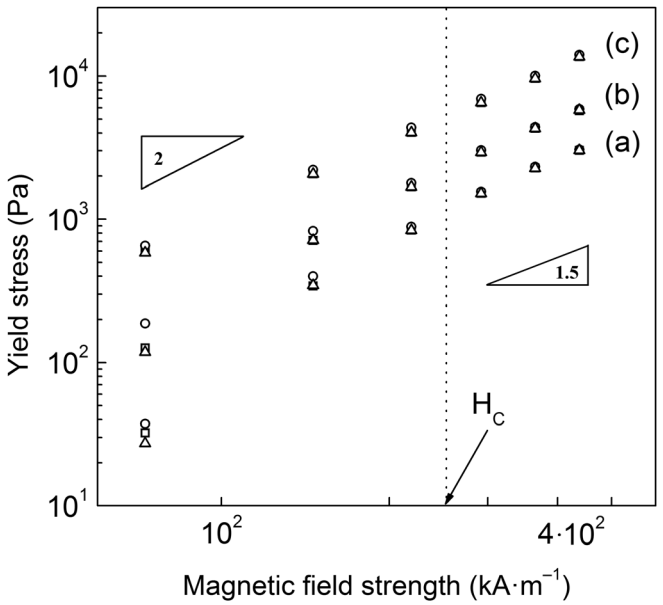

FIG. 7. Dynamic yield stresses of the MR suspensions based on 7.5 (a), 15 (b), and 30 vol. % (c) particle contents predicted according to the H–B (*open squares*), the R–S (*open circles*), and the M–B (*open up-triangles*) models as a function of magnetic field strength.

IV. CONCLUSION

In this work, the MR suspensions based on micron-sized, spherical CI particles were prepared and their steady shear behavior was studied under various magnetic field strengths. The ability of three-parameter rheological models—H–B, R–S, and M–B—to analyze experimental rheological data of MR suspensions was systematically investigated. The R–S and the M–B models commonly used in other research fields were successfully introduced to magnetorheology. It was established that the conventional H–B model tends to under-/overestimate the shear stress values. Based on the statistical evaluation, it was shown that the R–S model is a better alternative and can be considered as a more reliable analysis tool for the rheological data description of MR suspensions based on the spherical CI particles in a steady shear regime. The M–B model generally provided the lowest predictive/fitting capability. Considering the n parameter values, all models revealed pseudoplasticity in both diluted as well as concentrated MR suspensions upon the external magnetic field. The K parameter in the R–S model increased with the particle volume fraction and magnetic field strength, which was associated with the presence of more rigid internal structures in the system, while K parameter in the H–B and the M–B models varied randomly. Furthermore, it was found that the dynamic yield stresses predicted according to employed models were similar. Nevertheless, the yield stress obtained using the R–S model is seemingly the most accurate under defined conditions, as this model exhibited the closest fit to the experimental data.

ACKNOWLEDGMENT

This work was supported by the Ministry of Education, Youth and Sports of the Czech Republic—Program NPU I (LO1504).

References

[1] Bossis, G., S. Lacis, A. Meunier, and O. Volkova, "Magnetorheological fluids," J. Magn. Magn. Mater. **252**, 224–228 (2002).
[2] de Vicente, J., D. J. Klingenberg, and R. Hidalgo-Alvarez, "Magnetorheological fluids: A review," Soft Matter **7**, 3701–3710 (2011).
[3] Park, B. J., F. F. Fang, and H. J. Choi, "Magnetorheology: Materials and application," Soft Matter **6**, 5246–5253 (2010).
[4] Carlson, J. D., and M. R. Jolly, "MR fluid, foam and elastomer devices," Mechatronics **10**, 555–569 (2000).
[5] Kordonski, W., and A. Shorey, "Magnetorheological (MR) jet finishing technology," J. Intell. Mater. Syst. Struct. **18**, 1127–1130 (2007).
[6] Strecker, Z., J. Roupec, I. Mazurek, and M. Klapka, "Limiting factors of the response time of the magnetorheological damper," Int. J. Appl. Electromagn. Mech. **47**, 541–550 (2015).
[7] Wang, D. M., Y. F. Hou, and Z. Tian, "A novel high-torque magnetorheological brake with a water cooling method for heat dissipation," Smart Mater. Struct. **22**, 025019 (2013).
[8] Cvek, M., M. Mrlik, M. Ilcikova, J. Mosnacek, V. Babayan, Z. Kucekova, P. Humpolicek, and V. Pavlinek, "The chemical stability and cytotoxicity of carbonyl iron particles grafted with poly(glycidyl methacrylate) and the magnetorheological activity of their suspensions," RSC Adv. **5**, 72816–72824 (2015).
[9] Mrlik, M., M. Ilcikova, V. Pavlinek, J. Mosnacek, P. Peer, and P. Filip, "Improved thermooxidation and sedimentation stability of covalently-coated carbonyl iron particles with cholesteryl groups and their influence on magnetorheology," J. Colloid Interface Sci. **396**, 146–151 (2013).
[10] Lopez-Lopez, M. T., A. Zugaldia, F. Gonzalez-Caballero, and J. D. G. Duran, "Sedimentation and redispersion phenomena in iron-based magnetorheological fluids," J. Rheol. **50**, 543–560 (2006).
[11] Ghaffari, A., S. H. Hashemabadi, and M. Ashtiani, "A review on the simulation and modeling of magnetorheological fluids," J. Intell. Mater. Syst. Struct. **26**, 881–904 (2015).
[12] Wang, D. H., and W. H. Liao, "Magnetorheological fluid dampers: A review of parametric modelling," Smart Mater. Struct. **20**, 023001 (2011).
[13] de Vicente, J., F. Vereda, J. P. Segovia-Gutierrez, M. del Puerto Morales, and R. Hidalgo-Alvarez, "Effect of particle shape in magnetorheology," J. Rheol. **54**, 1337–1362 (2010).
[14] Farjoud, A., N. Vahdati, and Y. F. Fah, "Mathematical model of drum-type MR brakes using Herschel-Bulkley shear model," J. Intell. Mater. Syst. Struct. **19**, 565–572 (2008).
[15] Kittipoomwong, D., D. J. Klingenberg, and J. C. Ulicny, "Dynamic yield stress enhancement in bidisperse magnetorheological fluids," J. Rheol. **49**, 1521–1538 (2005).
[16] Ahmadkhanlou, F., M. Mahboob, S. Bechtel, and G. Washington, "An improved model for magnetorheological fluid-based actuators and sensors," J. Intell. Mater. Syst. Struct. **21**, 3–18 (2010).
[17] Kelessidis, V. C., and R. Maglione, "Modeling rheological behavior of bentonite suspensions as Casson and Robertson-Stiff fluids using Newtonian and true shear rates in Couette viscometry," Powder Technol. **168**, 134–147 (2006).
[18] Choi, H. J., T. M. Kwon, and M. S. Jhon, "Effects of shear rate and particle concentration on rheological properties of magnetic particle suspensions," J. Mater. Sci. **35**, 889–894 (2000).
[19] Sidpara, A., M. Das, and V. K. Jain, "Rheological characterization of magnetorheological finishing fluid," Mater. Manuf. Processes **24**, 1467–1478 (2009).
[20] Sayed-Ahmed, M. E., and A. S. El-Yazal, "Laminar fully developed flow and heat transfer of Robertson-Stiff fluids in a rectangular duct," Can. J. Phys. **83**, 165–182 (2005).

[21] Nunez-Santiago, M. C., E. Santoyo, L. A. Bello-Perez, and S. Santoyo-Gutierrez, "Rheological evaluation of non-Newtonian Mexican nixtamalised maize and dry processed masa flours," J. Food Eng. **60**, 55–66 (2003).
[22] Pelegrine, D. H., F. C. Silva, and C. A. Gasparetto, "Rheological behavior of pineapple and mango pulps," LWT—Food Sci. Technol. **35**, 645–648 (2002).
[23] Song, K. W., Y. S. Kim, and G. S. Chang, "Rheology of concentrated xanthan gum solutions: Steady shear flow behavior," Fibers Polym. **7**, 129–138 (2006).
[24] Barnes, H. A., "The yield stress—A review or 'rcavxa pst'—everything flows?," J. Non-Newtonian Fluid Mech. **81**, 133–178 (1999).
[25] Balhoff, M. T., L. W. Lake, P. M. Bommer, R. E. Lewis, M. J. Weber, and J. M. Calderin, "Rheological and yield stress measurements of non-Newtonian fluids using a Marsh Funnel," J. Pet. Sci. Eng. **77**, 393–402 (2011).
[26] Shorey, A. B., W. I. Kordonski, S. R. Gorodkin, S. D. Jacobs, R. F. Gans, K. M. Kwong, and C. H. Farny, "Design and testing of a new magnetorheometer," Rev. Sci. Instrum. **70**, 4200–4206 (1999).
[27] Laun, H. M., and C. Gabriel, "Measurement modes of the response time of a magnetorheological fluid (MRF) for changing magnetic flux density," Rheol. Acta **46**, 665–676 (2007).
[28] Jonkkari, I., E. Kostamo, J. Kostamo, S. Syrjala, and M. Pietola, "Effect of the plate surface characteristics and gap height on yield stresses of a magnetorheological fluid," Smart Mater. Struct. **21**, 075030 (2012).
[29] Kordonski, W., and S. Gorodkin, "The behavior of a magnetorheological (MR) fluid under compressive deformation," J. Rheol. **60**, 129–139 (2016).
[30] Khalil, M., B. M. Jan, and A. A. A. Raman, "Rheological and statistical evaluation of nontraditional lightweight completion fluid and its dependence on temperature," J. Pet. Sci. Eng. **77**, 27–33 (2011).
[31] Ngatu, G. T., N. M. Wereley, J. O. Karli, and R. C. Bell, "Dimorphic magnetorheological fluids: Exploiting partial substitution of microspheres by nanowires," Smart Mater. Struct. **17**, 045022 (2008).
[32] Vereda, F., J. de Vicente, J. P. Segovia-Gutierrez, and R. Hidalgo-Alvarez, "On the effect of particle porosity and roughness in magnetorheology," J. Appl. Phys. **110**, 063520 (2011).
[33] Filip, P., and J. David, "Axial Couette–Poiseuille flow of power-law viscoplastic fluids in concentric annuli," J. Pet. Sci. Eng. **40**, 111–119 (2003).
[34] Bailey, W. J., and I. S. Weir, "Investigation of methods for direct rheological model parameter estimation," J. Pet. Sci. Eng. **21**, 1–13 (1998).
[35] See supplementary material at http://dx.doi.org/10.1122/1.4954249 for summary of numerical results of rheological model parameters and statistical parameters for the MR suspensions based on different contents of the CI under various magnetic field strengths.
[36] Fang, F. F., H. J. Choi, and M. S. Jhon, "Magnetorheology of soft magnetic carbonyl iron suspension with single-walled carbon nanotube additive and its yield stress scaling function," Colloids Surf. A **351**, 46–51 (2009).
[37] Ginder, J. M., L. C. Davis, and L. D. Elie, "Rheology of magnetorheological fluids: Models and measurements," Int. J. Mod. Phys. B **10**, 3293–3303 (1996).